nature physics

Article

https://doi.org/10.1038/s41567-023-02141-0

Magnetic trapping of ultracold molecules at high density

Received: 20 November 2022

Accepted: 21 June 2023

Published online: 31 July 2023



Check for updates

Trapping ultracold molecules in conservative traps is essential for multiple applications, including quantum-state-controlled chemistry, quantum simulations and quantum information processing. The study of molecular collisions, in particular, requires samples at high densities, which have been challenging to achieve so far with established cooling and trapping techniques. Here we report the magnetic trapping of molecules in the triplet ground state at high density and ultralow temperature. We measure the inelastic loss rates in a single-spin sample and spin mixtures of fermionic molecules and spin-stretched atom-molecule mixtures. We demonstrate the sympathetic cooling of molecules in the magnetic trap by the radio-frequency evaporation of co-trapped atoms and observe an increase in the molecules' phase-space density by a factor of 16. Magnetic trapping at these densities allows the study of both atom-molecule and moleculemolecule collisions in the ultracold regime in the absence of trapping light, which often leads to undesired photochemistry effects.

Ultracold molecules offer new opportunities for quantum-statecontrolled chemistry^{1,2}, quantum simulations³⁻⁵ and quantum information processing⁶⁻⁹. For more than two decades, various methods were developed with the goal to trap molecular samples at densities high enough to study molecular collisions. Using buffer gas cooling 10-13 or Stark or magnetic deceleration¹⁴⁻¹⁶, molecules were trapped in magnetic traps in the temperature range of tens or hundreds of millikelvins. In only one case (O_2) were the densities high enough (estimated at ~10¹⁰ cm⁻³) to observe molecular collisions¹⁷. Dipolar molecules can be trapped with electric forces. Collisions between CH₃F molecules were observed in an electrostatic trap at densities of 10^7 cm⁻³ (ref. 18), and elastic collisions of OH were observed in an electromagnetic trap at temperatures of around 60 mK (ref. 19), although none of these studies reached the ultracold-temperature regime. Ultracold lasercooled molecules (in the 50-100 μK range) were transferred into magnetic traps at densities of $\lesssim 10^6$ cm⁻³ (refs. 20,21), which are too low for the observation of intermolecular collisions.

Optical traps have the advantages of trapping non-magnetic molecules and providing tight confinement, which has allowed the study of collisions involving molecules created by ultracold assembly or direct laser cooling. For example, collisional resonances have been observed in atom-molecule mixtures²²⁻²⁵ and between molecules²⁶ in optical traps. The disadvantage of optical traps is the small trapping volume and the presence of intense laser light, which can induce photochemistry. This has become a major concern recently after many experiments have found fast collisional losses even for non-reactive molecules, possibly due to 'sticky collisions' connected with long-lived complexes^{27–31}. Recent experiments to test these proposals suggest that optical traps can cause short lifetimes of molecules and are not truly conservative³²⁻³⁶, emphasizing the need for 'laser-free' trapping.

Here we report the magnetic trapping of triplet ²³Na⁶Li $(a^3\Sigma^+)$ molecules in the rovibrational ground state with high density (~10¹¹ cm⁻³) and ultracold temperature (~1 µK). The typical density is a factor of 105 higher compared with previous experiments with magnetically trapped ultracold molecular gases. Inelastic losses are detected in single component and spin mixtures of a fermionic NaLi molecular gas.

Another major long-standing goal has been the magnetic trapping of molecules together with atoms for the sympathetic cooling of molecules to achieve higher molecular densities or phase-space densities (PSDs)^{37,38}. The magnetic co-trapping of NH and N (ref. 39), and

Research Laboratory of Electronics, MIT-Harvard Center for Ultracold Atoms, Department of Physics, Massachusetts Institute of Technology, Cambridge, MA, USA. 2Institute for Quantum Computing and Department of Physics & Astronomy, University of Waterloo, Waterloo, Ontario, Canada. ⊠e-mail: jjpark@mit.edu

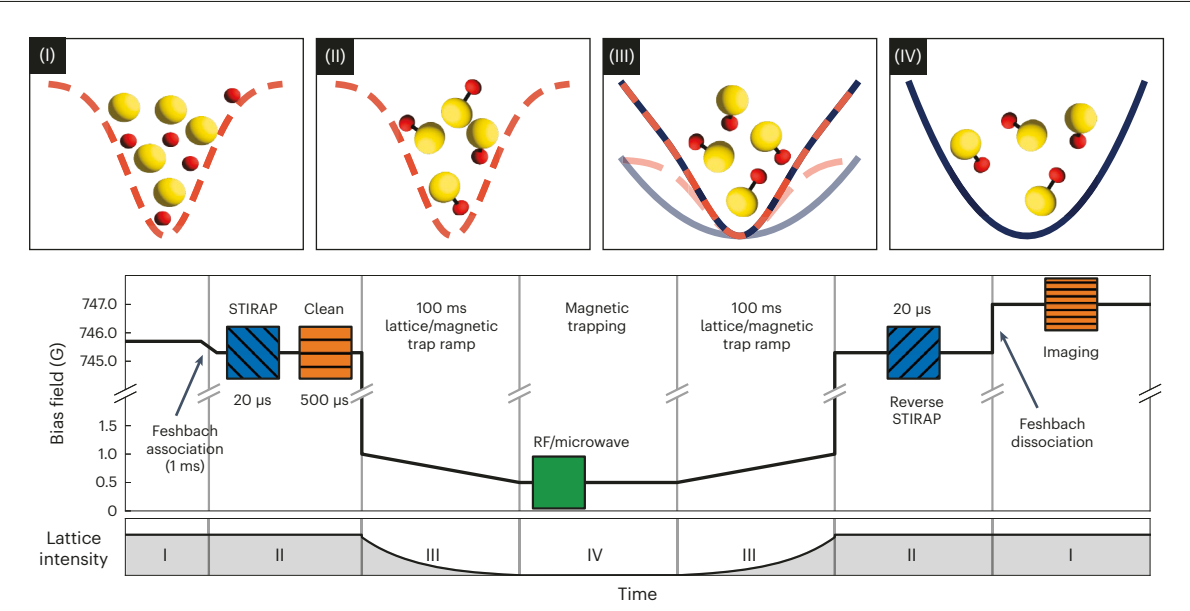


Fig. 1 | **Illustration of the experimental sequence.** The top panels show how atoms and molecules are confined in different traps. Na/Li mixture is confined in a 1D lattice potential (indicated with the orange dashed line) (I). NaLi molecules are trapped in the same 1D lattice (II). NaLi molecules are trapped in a hybrid trap created by a 1D lattice and a magnetic trap (indicated by the black line) (III). Molecules are purely confined by a magnetic trap (IV). The middle plot is the experimental sequence to produce and isolate NaLi molecules (the time axis is not to scale). The molecules are formed via Feshbach formation and STIRAP

in a 1D lattice, and the free atoms are removed using resonant light pulses at a high field. After the magnetic bias field is dropped to a low field, the lattice is ramped down and the magnetic trap is turned on in 100 ms. In the magnetic trap, RF or microwave is applied to the molecules for thermometry or preparation of molecular spin mixtures. For detection, the molecules are transferred back to the 1D lattice, the molecule formation process is reversed and the dissociated free atoms are imaged. The bottom row is the lattice intensity as a function of time along with the particle and trap type indicated using the indices I–IV.

more recently of CaF and Rb (ref. 40) and O_2 with Li atoms⁴¹, has been achieved. However, so far, only inelastic collisions were observed^{39,40}, with atomic densities far too low for sympathetic cooling.

Here we demonstrate the sympathetic cooling of molecules in a magnetic trap. We use a spin-stretched 23 Na 6 Li + 23 Na mixture, which had been used in another work 42 and observe an increase in the PSD of the molecular gas by more than an order of magnitude after the radio-frequency (RF) evaporation of Na atoms.

Experimental protocol and results

The experiments are carried out with NaLi molecules in the triplet ground state $(a^3\Sigma^+, \nu = 0, N = 0)$ created by means of the ultracold assembly of Na and Li atoms in the lowest-energy Zeeman states following the procedure described elsewhere 22,26,42. The procedure has been improved so that the Na/Li mixture is directly transferred from the initial magnetic trap into a 1,550 nm one-dimensional (1D) optical lattice without the use of extra optical traps (previous configurations required a 1,064 nm optical dipole trap and a 1,596 nm 1D optical lattice). After 0.4 s of forced evaporation of the atom mixture, 10⁵ molecules at 1.8 µK temperature are formed in the maximally stretched low-field-seeking hyperfine state ($|F_1 = 5/2, F = 7/2, m_F = 7/2\rangle$) using Feshbach association and Stimulated Raman adiabatic passage (STIRAP) transfer to the triplet ground state. Here *F* is the total angular momentum including electron and nuclear spins, m_F is the F projection to the quantization axis and F_1 is a good quantum number in the zero-field limit combining the electron spin and Na nuclear spin⁴³.

After ramping down the bias field from -745 G, where the association to molecules occurs, to a low magnetic bias field in 20 ms, the molecules are transferred from the optical lattice to an loffe–Pritchard magnetic trap with a depth of several millikelvins and a bias field of 0.56 G in 100 ms. The molecules are trapped for various hold times and transferred back to the optical lattice in 100 ms for detection at a high field (-745 G). The number of molecules is counted by absorption imaging of the Li atoms from the recaptured and dissociated molecules.

The experimental sequence is illustrated in Fig. 1. The transfer efficiency of molecules from the optical trap to the magnetic trap is close to 100%, whereas the recapture efficiency back to the optical trap is only about 50% due to a smaller optical trap volume.

We mainly investigate three types of inelastic collision: p-wave collisions in single-spin-component molecular gas, s-wave collisions in molecular spin mixtures and low-reactivity atom—molecule collisions, that is, NaLi + Na, in the low-field-seeking spin-stretched states. For this, the molecules in the hyperfine state $|F_1=5/2, F=7/2, m_F=7/2\rangle$ are held by the magnetic trap in the single-spin state, or together with molecules in another hyperfine state or Na atoms in the upper spin-stretched state ($|F=2, m_F=2\rangle$). The energy-level diagram of NaLi molecules in the triplet ground state is shown in Fig. 2a. We focus on the number decay of NaLi in state $|F_1=5/2, F=7/2, m_F=7/2\rangle$ in the magnetic trap.

Densities are obtained from an estimation of the magnetic trap volume. For this, we measure the trap frequencies for Na atoms in the upper spin-stretched state ($|F=2, m_F=2\rangle$) and the temperature of the upper stretched NaLi or Na atoms (Methods). The measured Na trap frequencies are $(f_x, f_y, f_z) = (282.0, 282.0, 14.8)$ Hz. For the thermometry of NaLi, we let the spin-polarized NaLi molecules in the $|F_1 = 5/2, F = 7/2, m_F = 7/2$ hyperfine state undergo RF-induced spin flips in the magnetic trap to map the density distribution of the molecules. RF is swept from some high value (>600 kHz) to various final RF values (RF knife frequencies) f in 600 ms (faster than collisional rethermalization timescales). This RF induces seven simultaneous resonant spin flips from $|F_1 = 5/2, F = 7/2, m_F = 7/2\rangle$ to $|F_1 = 5/2, F = 7/2, m_F = -7/2\rangle$, allowing the molecules to escape the trap (Fig. 2c, inset). The number of molecules remaining in the magnetic trap as a function of the RF knife frequency determines the density distribution of the molecular gas in the magnetic trap and therefore the temperature, too. Note that time-of-flight thermometry out of the magnetic trap is not possible, since before detection, the molecules have to be dissociated via reverse STIRAP and magnetic-field sweep across the Feshbach resonance. Due to the possible heating of molecules when transferring back to

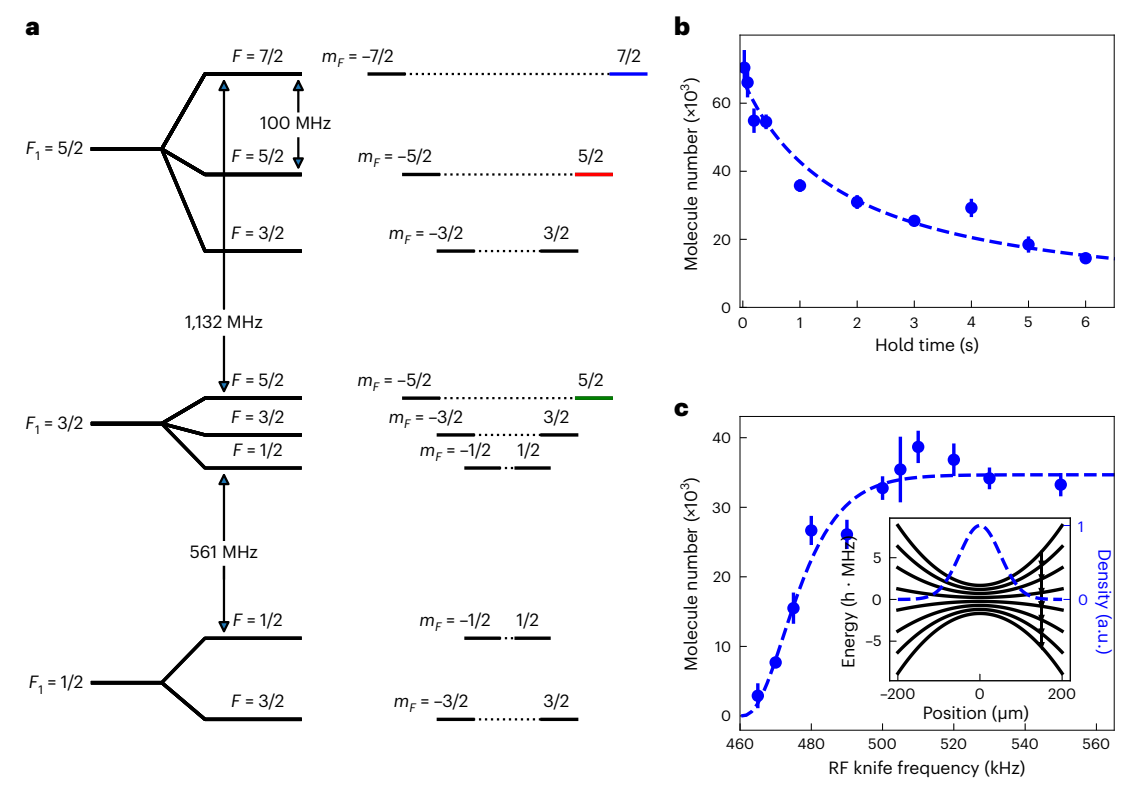


Fig. 2 | **Ground-state hyperfine structure of triplet NaLi and decay of spin-stretched molecules. a**, Rovibrational ground-state energy-level diagram of NaLi molecules in the triplet potential $(a^3\mathcal{D}^+)$ at zero bias field. Quantum number $F = |\vec{F}| = |\vec{S}| + \vec{I}_{Na} + \vec{I}_{Li}|$ is the total angular momentum, where $S = |\vec{S}| = 1$ is the total electron spin of NaLi and $I_{Na} = 3/2$ and $I_{Li} = 1$ are the nuclear spins of Na and Li, respectively. In the zero-field limit, $F_1 = |\vec{S}| + \vec{I}_{Na}| = 1/2, 3/2$, and 5/2 is an approximately good quantum number that characterizes the largest-scale hyperfine splittings as the hyperfine splitting due to the Na nucleus is substantially larger than that due to the Li nucleus. The molecules are initially formed in the low-field-seeking spin-polarized hyperfine state

 $(|F_1=5/2,F=7/2,m_F=7/2\rangle)$, as indicated in blue. The states in red and green are the other hyperfine states used for creating molecular spin mixtures. **b**, Number decay of low-field-seeking spin-polarized NaLi molecules $(|F_1=5/2,F=7/2,m_F=7/2\rangle)$ in a magnetic trap. **c**, Number of molecules left in the magnetic trap as a function of the RF knife frequency. The dashed line is a fitting function for a temperature of 1.01 μ K. The inset shows the m_F energy levels of NaLi in $|F_1=5/2,F=7/2\rangle$ near the centre of a magnetic trap (black lines). The example of the density profile of molecules in the top hyperfine state is shown in the blue dashed line. The data values represent the average and the error bars reflect one standard deviation of the mean of 3–7 measurements throughout the paper.

the optical lattice and the uncertainty of the optical trap geometry, thermometry using the temperature of the dissociated molecules is not reliable. The best estimate for the temperature of the other molecular spin component (indicated with NaLi*) is given by $T_{\rm NaLi} \approx T_{\rm NaLi} (\mu_{\rm NaLi} + 1)/2$, where $T_{\rm NaLi}$ is the temperature of NaLi in the upper stretched state and $\mu_{\rm NaLi} / \mu_{\rm NaLi}$ is the magnetic moment ratio (Methods). The Na temperature is directly measured from the time-of-flight absorption imaging out of the magnetic trap at a low field.

We first observe *p*-wave inelastic collisions of NaLi in the upper spin-stretched state. The number of molecules in the magnetic trap with a bias field of 0.56 G decays by more than 50% starting from 6×10^4 in a few seconds (Fig. 2b), whereas the typical vacuum lifetime is greater than 20 s. The molecular temperature is $1.01\pm0.18~\mu\text{K}$, which is measured by applying an RF knife of various frequencies (Fig. 2c). The initial density is $1.7\times10^{11}~\text{cm}^{-3}$ –a factor of 10^5 greater than the experiments carried out elsewhere 20,21 . The loss rate coefficient is calculated as $(3.3\pm1.4)\times10^{-12}~\text{(cm}^3~\text{s}^{-1})(T_{\text{NaLi}}~\mu\text{K}^{-1})$ from the best fit to a two-body loss model described elsewhere 26 (Methods).

Within the uncertainty, the measured loss rate is consistent with the value reported in another work²², which was measured for optically trapped NaLi in the upper spin-stretched state near 980 G. It is a factor of 2 larger than an estimated p-wave universal value, that is, $K_{l=1}^{\text{univ}}/T = (1.2 \pm 0.3) \times 10^{-12} \, \text{cm}^3 \, \text{s}^{-1} \, \mu \text{K}^{-1}$, which is obtained using an approximate value of the NaLi–NaLi long-range dispersion coefficient ($C_6 = 5.879 \, \text{a.u}$) estimated by summing all the C_6 coefficients between

the two constituent atoms⁴⁴. Due to this uncertainty, we consider our result to be consistent with the universal limit. Our observation of the universal limit in both optical trap and magnetic trap confirms the highly reactive nature of NaLi + NaLi collisions. In this case, the light-assisted decay of the collision complex will not enhance the loss rate further.

Next, we observe s-wave inelastic collisions by creating a spin mixture of molecules in two different hyperfine states. A transition from $|F_1 = 5/2, F = 7/2, m_F = 7/2\rangle$ to $|F_1 = 5/2, F = 5/2, m_F = 5/2\rangle$ is driven by 100 MHz RF until the molecules form a near-50/50 spin mixture in the magnetic trap. Similarly, the mixture of $|5/2, 7/2, 7/2\rangle$ and |3/2, 5/2,5/2) is prepared with a 1,133 MHz microwave drive. Due to magneticfield inhomogeneity, the superposition of the two spin states decoheres within $T_2 \approx \frac{h}{\Delta \mu \times \delta B} \lesssim 500 \ \mu s$, where $\Delta \mu$ is the magnetic moment difference between the two hyperfine states and $\delta B \approx 10$ mG is the magnetic-field inhomogeneity, during and after an approximate $\pi/2$ pulse. The loss rate coefficients are calculated to be $(3.3 \pm 1.5) \times 10^{-11}$ and $(1.0 \pm 0.4) \times 10^{-10}$ cm³ s⁻¹, respectively, by fitting the data in Fig. 3 to a loss model described in Methods. These values are about a factor of five and two lower than the s-wave universal value estimated using the approximate NaLi-NaLi long-range dispersion coefficient $(K_{l=0}^{\text{univ}} = 1.85 \times 10^{-10} \text{ cm}^3 \text{ s}^{-1})$, respectively, This suggests that nonuniversal losses can be highly state dependent for s-wave collisions. These non-universal losses in a chemically reactive system are

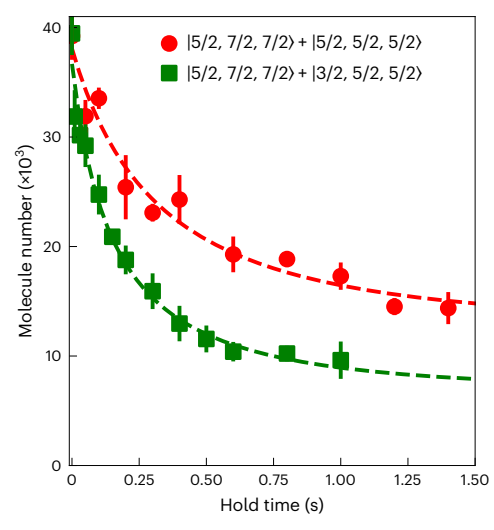


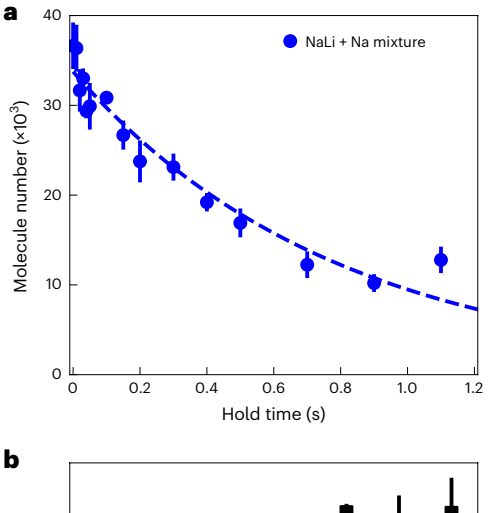
Fig. 3 | **Inelastic loss of molecular spin mixtures.** Number decay of low-field-seeking spin-polarized NaLi molecules ($|F_1 = 5/2, F = 7/2, m_F = 7/2\rangle$) when magnetically trapped together with molecules in state $|F_1 = 5/2, F = 5/2, m_F = 5/2\rangle$ (red circles) and $|F_1 = 3/2, F = 5/2, m_F = 5/2\rangle$ (green squares).

unexpected and warrant further theoretical studies. In addition, they open opportunities for searching for photoinduced trap loss and address interesting open questions on 'sticky collisions' connected with long-lived complexes²⁷⁻³¹.

For atom–molecule collisions, we load together about 4×10^5 Na atoms and about 4×10^4 NaLi in the upper stretched hyperfine states into the magnetic trap. The temperature of the atoms is -2 µK from time-of-flight imaging. Since the Na number is much greater than the NaLi number, we fit the molecule decay (Fig. 4a) to a simple exponential decay curve. The measured loss rate constant $\beta=(6.3\pm1.4)\times10^{-12}\,\mathrm{cm^3\,s^{-1}}$ is about a factor of 30 lower than the universal value $(1.72\times10^{-10}\,\mathrm{cm^3\,s^{-1}})$, which is well known for this system⁴⁵. Since only the quartet state of Na + NaLi is non-reactive, the loss rates are much higher for other combinations of hyperfine states⁴⁵, and this should also apply to Li + NaLi mixtures.

With the low-reactivity atom-molecule mixture, we demonstrate sympathetic cooling of molecules in the magnetic trap. Here, via RF-controlled evaporation, we have independent control over the molecule and atom trap depths. It is possible to cool spin-polarized NaLi using collisions with Na, also spin-polarized in the same direction as NaLi, because NaLi has a favourable ratio of elastic-to-inelastic collisions γ with Na. At a high field, it was measured to be $\gamma \approx 300$ (ref. 42). After loading the atom-molecule mixture into the magnetic trap, we slowly evaporate Na atoms out of the trap with a microwave sweep. We perform a microwave sweep to remove all the Na from the magnetic trap in 1 s, which is chosen to be similar to the lifetime of NaLi with Na and longer than the thermalization time among Na (-670 ms) and between Na and NaLi (-90 ms) (Methods).

We compare the temperature of NaLi after Na evaporation with that of NaLi from an identical mixture loaded into the magnetic trap but with the sudden removal of Na using a resonant light pulse after the loading. The two temperatures are estimated by the RF knife frequency scan described earlier (Fig. 4b). The evaporation of Na leads to a temperature of NaLi molecules of $0.8(1) \mu K$, substantially lower than the temperature without the evaporation (2.3(3) μK), whereas the molecule number is decreased by 30%. This corresponds to an increase in the PSD of the molecular gas by a factor of -16. The temperature T/T_F of NaLi in the magnetic trap is about 8.2 and 3.2 without and with the Na RF evaporation, respectively. These values are higher than the initial $T/T_F \approx 2.6$ of molecules without Na atoms (Fig. 2b,c). The difference is caused by the heating of Na atoms during



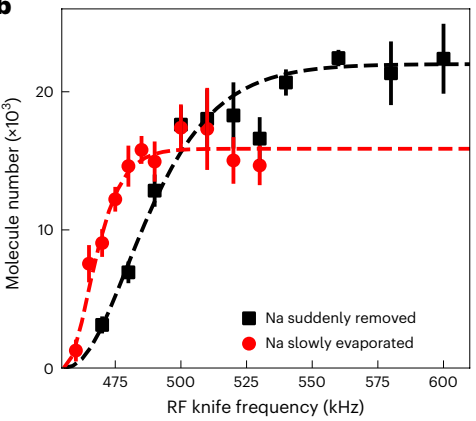


Fig. 4 | **Sympathetic cooling of NaLi by Na atoms. a**, Molecule number as a function of hold time in a magnetic trap when trapped together with Na. The atom–molecule mixture is in the low-field-seeking spin-stretched state. The Na number is about 4×10^5 and the temperature is $-2~\mu$ K. **b**, Molecule number as a function of RF knife frequency. Data in red circles are with slow evaporation of Na and data in black squares are with Na suddenly removed after loading into a magnetic trap. The density profile obtained from the red (black) data implies a temperature of $0.8(1)~\mu$ K ($2.3(3)~\mu$ K). The fits in the dashed lines use a fit function (Methods).

the non-adiabatic transfer to the magnetic trap. Without this heating process, a much lower final $T/T_F \approx 1$ is expected after the RF evaporation step.

Outlook

In summary, we have shown the magnetic trapping of molecules with a factor of 10^5 higher density compared with ultracold molecules previously studied in a magnetic trap. We have measured the inelastic collision rates for two selected molecular spin mixtures and a spin-stretched Na + NaLi mixture that serve as prototypes for future studies on state-dependent molecule–molecule and atom–molecule collisions in the magnetic trap. A quantitative analysis of molecular collisions in the magnetic trap is much simpler than in optical traps, because the magnetic trap is well approximated by a harmonic potential whose trap frequencies are determined by molecule magnetic moments, which are typically well known. In contrast, optical traps can be highly anharmonic near the top of the trap, and ratios of trap frequencies (unless directly measured) can be difficult to determine because of the unknown molecular a.c. polarizability.

Our collisional studies show that NaLi molecules with various collision partners have loss rates far below the universal limit. Although all the collision systems are reactive, the absorption probability at a close range is much smaller than one. This is well understood for the

collisions in the spin-stretched Na + NaLi mixture^{22,46}, where the quartet potential in the input channel is non-reactive, and inelastic collisions are only possible via spin flips. However, this explanation does not apply to the s-wave molecule-molecule collisions studied here. Also, a molecule-molecule Feshbach resonance has been observed for a strongly reactive input potential²⁶. These observations suggest that collisional resonances and collisional complexes should occur more generally, and motivate more systematic studies of collisions involving NaLi and collision partners in various hyperfine states, as well as for other molecules⁴⁷. We also demonstrated the sympathetic cooling of NaLi by the RF evaporation of Na atoms, increasing the PSD of the molecules by a factor of ~16. This can be further optimized, but is eventually limited by the slow Nathermalization rate, which is substantially slower than the rate of elastic collisions between Na and NaLi. One solution is to superimpose a second trap with a wavelength chosen such that it mainly acts on Na atoms. This trap could enhance the thermalization rate of Na atoms and suppress the inelastic collisions with NaLi by reducing overlap between the two clouds. This should allow cooling into the quantum-degenerate regime.

Our new method now allows studies of molecular collisions in a photon-free environment. Experiments probing photoinduced loss for ultracold molecular systems in optical traps have been reported using chopped optical dipole traps or repulsive box potentials made with blue-detuned light. However, even for the longest dark times and the lowest intensities, photoinduced loss could not be completely suppressed, and loss rates consistent with universal loss were observed 34-36. For magnetically trapped molecules, photoinduced losses can be studied with arbitrarily small light intensities. In addition, stable microwave-induced dipoles or rotational state qubits can be achieved with technical upgrades to our apparatus. The most stable rotational qubits that have been reported are limited by the differential polarizability between two qubit states⁴⁸. In contrast, in the light-free magnetic trap, decoherence is slow because it is caused by the rotational state-dependent differential magnetic moment, which is small. In a previous experiment with CaF, the 6 ms coherence time was limited by the high temperature of the molecules and the inhomogeneous quadrupole field⁴⁹. For the conditions achieved in our work, we expect to produce dipoles with a coherence time of 200 ms, which is longer than the longest previously observed coherence time.

Online content

Any methods, additional references, Nature Portfolio reporting summaries, source data, extended data, supplementary information, acknowledgements, peer review information; details of author contributions and competing interests; and statements of data and code availability are available at https://doi.org/10.1038/s41567-023-02141-0.

References

- Krems, R. V. Cold controlled chemistry. Phys. Chem. Chem. Phys. 10, 4079–4092 (2008).
- Balakrishnan, N. Perspective: ultracold molecules and the dawn of cold controlled chemistry. J. Chem. Phys. 145, 150901 (2016).
- Micheli, A., Brennen, G. & Zoller, P. A toolbox for lattice-spin models with polar molecules. Nat. Phys. 2, 341–347 (2006).
- Capogrosso-Sansone, B., Trefzger, C., Lewenstein, M., Zoller, P. & Pupillo, G. Quantum phases of cold polar molecules in 2D optical lattices. *Phys. Rev. Lett.* **104**, 125301 (2010).
- Blackmore, J. A. et al. Ultracold molecules for quantum simulation: rotational coherences in CaF and RbCs. Quantum Sci. Technol. 4, 014010 (2018).
- Ni, K.-K., Rosenband, T. & Grimes, D. D. Dipolar exchange quantum logic gate with polar molecules. Chem. Sci. 9, 6830–6838 (2018).
- Herrera, F., Cao, Y., Kais, S. & Whaley, K. B. Infrared-dressed entanglement of cold open-shell polar molecules for universal matchgate quantum computing. New J. Phys. 16, 075001 (2014).

- Hughes, M. et al. Robust entangling gate for polar molecules using magnetic and microwave fields. *Phys. Rev. A* **101**, 062308 (2020).
- 9. Sawant, R. et al. Ultracold polar molecules as qudits. *New J. Phys.* **22**, 013027 (2020).
- Weinstein, J. D., DeCarvalho, R., Guillet, T., Friedrich, B. & Doyle, J. M. Magnetic trapping of calcium monohydride molecules at millikelvin temperatures. *Nature* 395, 148–150 (1998).
- Campbell, W. C., Tsikata, E., Lu, H.-I., van Buuren, L. D. & Doyle, J. M. Magnetic trapping and Zeeman relaxation of NH (X³Σ⁻).
 Phys. Rev. Lett. 98, 213001 (2007).
- Lu, H.-I., Kozyryev, I., Hemmerling, B., Piskorski, J. & Doyle, J. M. Magnetic trapping of molecules via optical loading and magnetic slowing. *Phys. Rev. Lett.* 112, 113006 (2014).
- Tsikata, E., Campbell, W., Hummon, M., Lu, H.-I. & Doyle, J. M. Magnetic trapping of NH molecules with 20s lifetimes. New J. Phys. 12, 065028 (2010).
- Liu, Y., Zhou, S., Zhong, W., Djuricanin, P. & Momose, T. One-dimensional confinement of magnetically decelerated supersonic beams of O₂ molecules. *Phys. Rev. A* 91, 021403 (2015).
- Liu, Y. et al. Magnetic trapping of cold methyl radicals. *Phys. Rev. Lett.* 118, 093201 (2017).
- Riedel, J. et al. Accumulation of Stark-decelerated NH molecules in a magnetic trap. Eur. Phys. J. D 65, 161–166 (2011).
- Segev, Y. et al. Collisions between cold molecules in a superconducting magnetic trap. Nature 572, 189–193 (2019).
- Koller, M. et al. Electric-field-controlled cold dipolar collisions between trapped CH₃F molecules. *Phys. Rev. Lett.* 128, 203401 (2022)
- Reens, D., Wu, H., Langen, T. & Ye, J. Controlling spin flips of molecules in an electromagnetic trap. *Phys. Rev. A* 96, 063420 (2017).
- 20. McCarron, D., Steinecker, M., Zhu, Y. & DeMille, D. Magnetic trapping of an ultracold gas of polar molecules. *Phys. Rev. Lett.* **121**, 013202 (2018).
- 21. Williams, H. et al. Magnetic trapping and coherent control of laser-cooled molecules. *Phys. Rev. Lett.* **120**, 163201 (2018).
- 22. Son, H. et al. Control of reactive collisions by quantum interference. *Science* **375**, 1006–1010 (2022).
- Park, J. J. et al. Spectrum of Feshbach resonances in NaLi+Na collisions. Preprint at arXiv https://doi.org/10.48550/arXiv. 2303.00863 (2023).
- Yang, H. et al. Observation of magnetically tunable Feshbach resonances in ultracold ²³Na⁴⁰K+⁴⁰K collisions. Science 363, 261–264 (2019).
- 25. Wang, X.-Y. et al. Magnetic Feshbach resonances in collisions of ²³Na⁴⁰K with ⁴⁰K. *New J. Phys.* **23**, 115010 (2021).
- Park, J. J., Lu, Y.-K., Jamison, A. O., Tscherbul, T. V. & Ketterle, W. A Feshbach resonance in collisions between triplet ground-state molecules. *Nature* 614, 54–58 (2023).
- Mayle, M., Ruzic, B. P. & Bohn, J. L. Statistical aspects of ultracold resonant scattering. *Phys. Rev. A* 85, 062712 (2012).
- Mayle, M., Quéméner, G., Ruzic, B. P. & Bohn, J. L. Scattering of ultracold molecules in the highly resonant regime. *Phys. Rev. A* 87, 012709 (2013).
- 29. Christianen, A., Karman, T. & Groenenboom, G. C. Quasiclassical method for calculating the density of states of ultracold collision complexes. *Phys. Rev. A* **100**, 032708 (2019).
- 30. Christianen, A., Zwierlein, M. W., Groenenboom, G. C. & Karman, T. Photoinduced two-body loss of ultracold molecules. *Phys. Rev. Lett.* **123**, 123402 (2019).
- 31. Liu, Y. & Ni, K.-K. Bimolecular chemistry in the ultracold regime. *Annu. Rev. Phys. Chem.* **73**, 73–96 (2022).
- 32. Liu, Y. et al. Photo-excitation of long-lived transient intermediates in ultracold reactions. *Nat. Phys.* **16**, 1132–1136 (2020).

- Gregory, P. D., Blackmore, J. A., Bromley, S. L. & Cornish, S. L. Loss of ultracold Rb⁸⁷Cs¹³³ molecules via optical excitation of long-lived two-body collision complexes. *Phys. Rev. Lett.* 124, 163402 (2020).
- Gregory, P. D. et al. Molecule–molecule and atom–molecule collisions with ultracold RbCs molecules. New J. Phys. 23, 125004 (2021).
- 35. Gersema, P. et al. Probing photoinduced two-body loss of ultracold nonreactive bosonic ²³Na⁸⁷Rb and ²³Na³⁹K molecules. *Phys. Rev. Lett.* **127**, 163401 (2021).
- Bause, R. et al. Collisions of ultracold molecules in bright and dark optical dipole traps. Phys. Rev. Research 3, 033013 (2021).
- Lara, M., Bohn, J. L., Potter, D., Soldán, P. & Hutson, J. M. Ultracold Rb-Oh collisions and prospects for sympathetic cooling. *Phys. Rev. Lett.* 97, 183201 (2006).
- Żuchowski, P. S. & Hutson, J. M. Prospects for producing ultracold NH₃ molecules by sympathetic cooling: a survey of interaction potentials. *Phys. Rev. A* 78, 022701 (2008).
- 39. Hummon, M. T. et al. Cold N+NH collisions in a magnetic trap. *Phys. Rev. Lett.* **106**, 053201 (2011).
- Jurgilas, S. et al. Collisions between ultracold molecules and atoms in a magnetic trap. Phys. Rev. Lett. 126, 153401 (2021).
- 41. Akerman, N. et al. Trapping of molecular oxygen together with lithium atoms. *Phys. Rev. Lett.* **119**, 073204 (2017).
- Son, H., Park, J. J., Ketterle, W. & Jamison, A. O. Collisional cooling of ultracold molecules. *Nature* 580, 197–200 (2020).
- Rvachov, T. M. et al. Long-lived ultracold molecules with electric and magnetic dipole moments. *Phys. Rev. Lett.* 119, 143001 (2017).

- Derevianko, A., Babb, J. & Dalgarno, A. High-precision calculations of van der Waals coefficients for heteronuclear alkali-metal dimers. *Phys. Rev. A* 63, 052704 (2001).
- Hermsmeier, R., Kłos, J., Kotochigova, S. & Tscherbul, T. V.
 Quantum spin state selectivity and magnetic tuning of ultracold chemical reactions of triplet alkali-metal dimers with alkali-metal atoms. *Phys. Rev. Lett.* 127, 103402 (2021).
- Tomza, M., Madison, K. W., Moszynski, R. & Krems, R. V. Chemical reactions of ultracold alkali-metal dimers in the lowest-energy ³Σ state. *Phys. Rev. A* 88, 050701 (2013).
- Voges, K. K., Gersema, P., Hartmann, T., Ospelkaus, S. & Zenesini, A. Hyperfine dependent atom-molecule loss analyzed by the analytic solution of few-body loss equations. *Phys. Rev. Research* 4. 023184 (2022).
- 48. Burchesky, S. et al. Rotational coherence times of polar molecules in optical tweezers. *Phys. Rev. Lett.* **127**, 123202 (2021).
- 49. Caldwell, L. et al. Long rotational coherence times of molecules in a magnetic trap. *Phys. Rev. Lett.* **124**, 063001 (2020).

Publisher's note Springer Nature remains neutral with regard to jurisdictional claims in published maps and institutional affiliations.

Springer Nature or its licensor (e.g. a society or other partner) holds exclusive rights to this article under a publishing agreement with the author(s) or other rightsholder(s); author self-archiving of the accepted manuscript version of this article is solely governed by the terms of such publishing agreement and applicable law.

© Springer Nature Limited 2023

Methods

Thermometry of molecules

We determine the temperature of a NaLi gas in the magnetic trap from its density profile. To find this, we let NaLi molecules in the $|F_1=5/2,F=7/2,m_F=7/2\rangle$ hyperfine state undergo RF-induced spin flips in a magnetic trap that has a trap bottom of 0.56 G. RF is swept from some high value (>600 kHz) to a lower value f in 600 ms. This RF can induce seven simultaneous transitions, by one quantum of m_F each, from state $|F_1=5/2,F=7/2,m_F=7/2\rangle$ to $|F_1=5/2,F=7/2,m_F=-7/2\rangle$, allowing the molecules to escape from the trap. The number of molecules left in the magnetic trap is determined by the final RF value (RF knife frequency). The maximum possible energy of the molecules is $A=\frac{7}{2}h(f-f_0)$, where f is the RF knife frequency and f_0 is the transition frequency from $|F_1=5/2,F=7/2,m_F=7/2\rangle$ to $|F_1=5/2,F=7/2,m_F=5/2\rangle$ at the bottom of the magnetic trap.

Near the centre, the magnetic field of the loffe–Pritchard magnetic trap varies quadratically with the distance from the origin. The states of the particles are enumerated by a set of quantum numbers $[n_x, n_y, n_z]$ in a general three-dimensional harmonic trap potential $V(x,y,z)=\frac{1}{2}m(\omega_x^2x^2+\omega_y^2y^2+\omega_z^2z^2)$ and the energy of a particular state is given by $\epsilon=\hbar(n_x\omega_x+n_y\omega_y+n_z\omega_z)+\epsilon_0$, where $\epsilon_0=\frac{1}{2}\hbar(\omega_x+\omega_y+\omega_z)$ is the zero-point energy in this harmonic trap. For $\epsilon\gg\epsilon_0$, the number of states with energy between ϵ and $\epsilon+d\epsilon$ is estimated as $g(\epsilon)d\epsilon$: $g(\epsilon)=\frac{\epsilon^2}{2\hbar^3\omega^3}$, where $\bar{\omega}=(\omega_x\times\omega_y\times\omega_z)^{1/3}$ is the geometric mean of the trap angular frequencies. Therefore, the particle number with energy between 0 and A is

$$N(A) = N_{\text{tot}} \frac{\int_0^A g(\epsilon) e^{-\beta \epsilon} d\epsilon}{\int_0^\infty g(\epsilon) e^{-\beta \epsilon} d\epsilon}$$
 (1)

$$= \frac{N_{\rm tot}}{2} \left[e^{-\beta A} \{ -\beta A \times (\beta A + 2) - 2 \} + 2 \right], \tag{2}$$

where $\beta = (k_{\rm B}T)^{-1}$ is the Boltzmann factor and $N_{\rm tot}$ is the total particle number. Fitting the data in Fig. 2c, which is the NaLi number as a function of the RF knife frequency f, into equation (2) provides the estimate for the molecule temperature of $1.06 \pm 0.18 \, \mu \text{K}$.

For the temperature estimation of NaLi in the other hyperfine state $(|F_1=5/2,F=5/2,m_F=5/2\rangle)$ of $|F_1=3/2,F=5/2,m_F=5/2\rangle)$ of a molecular spin mixture, we assume that the average total kinetic energy and the average total potential energy are equal in the harmonic trap by the virial theorem. After molecules are transferred from the upper stretched state to the other hyperfine state, the average potential energy of NaLi is momentarily reduced by the magnetic moment ratio $\mu_{\text{NaLi}}/\mu_{\text{NaLi}}$, whereas the kinetic energy remains the same. Here NaLi represents the upper stretched state and NaLi* indicates the other hyperfine state. The average potential and kinetic energy redistribute to be equal. With this simple model, the temperature is estimated as $T_{\text{NaLi}} \approx T_{\text{NaLi}}/\mu_{\text{NaLi}}/\mu_{\text{NaLi}}+1)/2$.

Decay models

The differential equations that describe the decay of molecules in the upper stretched state in the presence of another type of particle *i* are given as

$$\dot{N}_{\text{NaLi}} = -(K_i/V_{\text{ov}})N_iN_{\text{NaLi}} - (\beta_0/V_{\text{eff,NaLi}})N_{\text{NaLi}}^2, \tag{3}$$

$$\dot{N}_i = -(K_i/V_{\text{ov}})N_{\text{NaLi}}N_i - (\beta_i/V_{\text{eff},i})N_i^2, \tag{4}$$

where $N_{\rm NaLi}$ represents the number of NaLi in the upper stretched state and N_i represents the number of particles of type i that are magnetically trapped with the molecules. Here $V_{\rm ov}$ is the volume of the regime where the i-type particles overlap with the upper stretched molecules, $V_{\rm eff,}i$ is the mean volume filled with i-type particles, β_0 (β_i)

is the two-body molecular (particle i) loss rate coefficient and K_i is the loss rate coefficient for the collisions of i + NaLi pairs.

We solve the given differential equations for three different conditions: $N_i = 0$, $N_i \approx N_{\text{NaLi}}$ and $N_i \gg N_{\text{NaLi}}$. The two-body loss in the single-spin-component ($|F_1 = 5/2, F = 7/2, m_F = 7/2\rangle$) molecular gas, that is, $N_i = 0$, is described by the second term of equation (3) only. The analytical solution is given as $N_{\text{NaLi}}(t) = N_0 \frac{1}{1 + \beta_0 N_0 t/V_{\text{eff}}}$, where N_0 is the initial NaLi number.

For collisions in two-component mixtures that we experimentally study, the decay of the NaLi number is well described by equations (3) and (4) with the second terms approximated to zero since β_0 , $\beta_i \ll K_i$. With this approximation, the analytical solution becomes

$$N_{\text{NaLi}}(t) = \frac{D}{Ce^{D\Gamma t} - 1},\tag{5}$$

$$N_i(t) = -\frac{D}{\frac{1}{c}e^{-D\Gamma t} - 1},\tag{6}$$

where $\Gamma = K_i N_i(0)/V_{ov}$ is the loss rate, $C = N_i(0)/N_{NaLi}(0)$ and $D = N_i(0) - N_{NaLi}(0)$. In a regime where $N_i(0) \gg N_{NaLi}(0)$ in a two-component mixture, $N_i(t)$ can be approximated to $N_i(0)$ throughout and equation (5) is reduced to a simple exponential decay, namely, $N_{NaLi}(t) = N_0 e^{-K_i t/V_{ov}}$. In the experiment, the Na atom number was more than a factor of 10 larger than the NaLi molecule number, so the decay of NaLi is well described by the exponential function.

Now we discuss the volumes V_{eff} and V_{ov} in equations (3) and (4). Assuming a harmonic trap, one obtains

$$\begin{split} V_{\text{eff},i} &= \bar{\omega}_{i}^{-3} (4\pi k_{\text{B}} T_{i}/m_{i})^{3/2}, \\ V_{\text{OV}} &= \frac{N_{i}N_{\text{NaLi}}}{\int dV n_{i}n_{\text{NaLi}}} \\ &= \bar{\omega}_{\text{Na}}^{-3} \left[\left(\frac{2\pi k_{\text{B}} T_{i}}{m_{i}} \right) \left(\frac{\mu_{\text{Na}}}{\mu_{i}} + \frac{\mu_{\text{Na}}}{\mu_{i}} \frac{T_{\text{NaLi}}}{T_{i}} \right) \right]^{3/2}, \end{split}$$

where the geometric mean of the Na trap angular frequencies is $\bar{\omega}_{\mathrm{Na}} = (\omega_x \omega_y \omega_z)^{1/3} = 2\pi \times (282 \times 282 \times 14.8)^{1/3} \, \mathrm{Hz} \approx 2\pi \times 106 \, \mathrm{Hz}$. Here, n_i is the density, T_i is the temperature, m_i is the mass and μ_i is the magnetic moment of the type i particle. The geometric mean of the trap angular frequencies for NaLi in the upper stretched state is $\bar{\omega}_{\mathrm{NaLi}} = \bar{\omega}_{\mathrm{Na}} \times (m_{\mathrm{Na}}/m_{\mathrm{NaLi}}) \times (\mu_{\mathrm{NaLi}}/\mu_{\mathrm{Na}})$ where the mass ratio is $m_{\mathrm{NaLi}}/m_{\mathrm{Na}} \approx 29/23$ and the magnetic moment ratio is $\mu_{\mathrm{NaLi}}/\mu_{\mathrm{Na}} \approx 2$.

Inelastic collision and thermalization rates

To investigate the limiting factor for sympathetic cooling, we compare the three relevant timescales in a Na + NaLi mixture: the inelastic collision and thermalization rates between Na and NaLi, and the thermalization rate among Na atoms. The experiment was done with about 33×10^3 NaLi and 420×10^3 Na at a temperature of -2 μK in a magnetic trap. The initial densities of Na and NaLi are 1.25×10^{11} and 3.30×10^{10} cm $^{-3}$, respectively. The initial inelastic collision rate is experimentally measured to be $\varGamma_{\text{inel}}\approx1.2\,\text{s}^{-1}$ (Fig. 4a).

Next, we estimate the thermalization rate between Na and NaLi. In a mass-imbalanced system, the factor $3/\xi$ quantifies the approximate average number of collisions per particle required for thermalization, where $\xi = 4m_{\rm Na}m_{\rm NaLi}/(m_{\rm Na}+m_{\rm NaLi})^2\approx 0.987$ (refs. 42,50). Thus, the relation between the thermalization rate and elastic scattering rate is given by $\Gamma_{\rm th} \approx \Gamma_{\rm el}/(3/\xi)$. In our system, where the particle number is largely imbalanced, we can write the thermalization rate as

$$\Gamma_{\rm th} \approx \frac{(N_{\rm Na}/V_{\rm ov})\sigma_{\rm el}\nu_{\rm rel}}{3/\xi},$$
 (7)

where $N_{\rm Na}/V_{\rm ov}$ is the average density of Na atoms seen by NaLimolecules, $\sigma_{\rm el}$ is the elastic scattering cross section and relative velocity is $v_{\rm rel} = \sqrt{\frac{8k_{\rm B}}{\pi}\left(\frac{T_{\rm Na}}{m_{\rm Na}} + \frac{T_{\rm NaLi}}{m_{\rm NaLi}}\right)}$. The s-wave elastic scattering cross section

between Na and NaLi is given by $\sigma_{\rm el} \approx 4\pi a^2$, where a is the scattering length. Using an approximate value for the scattering length $a = 263(66)a_0$, where a_0 is the Bohr radius⁴², the thermalization rate is estimated to be -11 s⁻¹.

Similarly, the thermalization rate among Na is given as $\tilde{\Gamma}_{th} = \frac{(N_{Na}/V_{eff,Na})\sigma_{el}\tilde{\sigma}_{rel}}{3} \approx 1.5~\text{s}^{-1}$, where the s-wave elastic scattering cross section between Na atoms is $\tilde{\sigma}_{el} \approx 8\pi\tilde{\alpha}^2$, where the scattering length between Na atoms is $\tilde{\alpha} = 85(3)a_0$ (ref. 51). The relative velocity is $\tilde{\sigma}_{rel} = \sqrt{\frac{16k_B}{\pi}} \frac{T_{Na}}{m_{Na}}$. We see that $\Gamma_{inel} \approx \tilde{\Gamma}_{th} \ll \Gamma_{th}$, and the sympathetic cooling of NaLi is limited by the slow Na thermalization rate.

Data availability

The data that support the findings of this study are available from the corresponding author upon reasonable request.

Code availability

The codes used to generate the results are available from the corresponding author upon reasonable request.

References

- 50. Mosk, A. et al. Mixture of ultracold lithium and cesium atoms in an optical dipole trap. *Appl. Phys. B* **73**, 791–799 (2001).
- 51. Tiesinga, E. et al. A spectroscopic determination of scattering lengths for sodium atom collisions. *J. Res. Natl Inst. Stand. Technol.* **101**, 505–520 (1996).

Acknowledgements

We thank J. Doyle for valuable discussions. We acknowledge support from the National Science Foundation through grant no. PHY-1734011 for the Center for Ultracold Atoms and through grant no. 1506369, and from the Air Force Office of Scientific Research (MURI, grant no. FA9550-21-1-0069). Some of the analysis was performed by W.K. at the Aspen Center for Physics, which is supported by the National Science Foundation grant PHY-1607611. J.J.P. acknowledges additional support from the Samsung Scholarship.

Author contributions

J.J.P. and Y.-K.L. carried out the experimental work. All authors contributed to the development of models, data analysis and writing of the manuscript.

Competing interests

The authors declare no competing interests.

Additional information

Correspondence and requests for materials should be addressed to Juliana J. Park.

Peer review information *Nature Physics* thanks the anonymous reviewers for their contribution to the peer review of this work.

Reprints and permissions information is available at www.nature.com/reprints.